Smart Materials in Manufacturing 3 (2025) 100073

Contents lists available at ScienceDirect

Smart Materials in Manufacturing

journal homepage: www.keaipublishing.com/en/journals/smart-materials-in-manufacturing

Research Paper

Unveiling the structure-property relationships of multilayered Helmholtz resonance-based acoustic metamaterials

Jun Wei Chua [a], David Kar Wei Poh [a], Shuwei Ding [a], Haoran Pei [a,b], Xinwei Li [c,*]

[a] Department of Mechanical Engineering, National University of Singapore, Singapore, 117575
[b] State Key Laboratory of Polymer Materials Engineering, Polymer Research Institute of Sichuan University, Chengdu, 610065, China
[c] Faculty of Science, Agriculture, and Engineering, Newcastle University, Singapore, 567739

ARTICLE INFO

Keywords:
Lattice structures
Acoustic metamaterial
Sound absorption
Helmholtz resonators
Structure-property relationships

ABSTRACT

The principle of Helmholtz resonance has been widely employed in the design of sound-absorbing metamaterials. However, the relationship between various acoustic parameters and sound absorption performance remains insufficiently understood. This work investigates the effect of various structural parameters of multi-layered Helmholtz resonators (MLHRs) on sound absorption properties from a statistical point of view. The Taguchi method was used in the study with the pore diameter, pore thickness, and cavity depth of a layer of Helmholtz resonator as control variables and the number of layers of resonators as the noise variable. Results revealed a clear hierarchy of importance for maximizing sound absorption: increasing the number of layers, reducing pore diameter, enhancing pore thickness, and expanding cavity depth. Additionally, it is also found that the influence of the number of layers on said relationships was greatest with smaller pore diameters larger pore thicknesses, and cavity depths. All three control variables showed significant effects on the sound absorption properties of MLHRs when the number of layers was more than two, while the cavity width showed limited influence on sound absorption coefficients for a two-layer MLHR. This work provides a foundational understanding of the structural-property relationships in MLHRs, paving the way for optimized designs to achieve optimal sound absorption performance.

1. Introduction

Noise pollution is a recurring and increasingly severe problem in the urban environment. A study on the measurement of environmental noise in Singapore concluded that more than 90 percent of noise measurements in the daytime exceed the WHO recommended level of 55 dBA to minimize negative non-auditory health effects due to noise [1]. It was known that prolonged exposure to loud and unwanted noise results in several chronic physical and mental health issues such as irreversible hearing loss, sleep disturbances, cardiovascular disturbances, negative social behavior, and increased anxiety and stress [2]. The awareness of this problem has led to an increase in demand for acoustics materials for the manipulation of acoustic environments [3]. Traditional and commercial sound absorbers that make up the market have always been focused on foams, fibrous materials, fabric, and perforated panels [4]. Recently, there has been a rapidly increasing interest in the research and development of acoustic metamaterials to address these shortcomings. These metamaterials are artificial, engineered structures designed to control sound propagation by controlling their effective mass densities and bulk moduli [5]. Particularly, multi-layered Helmholtz resonators (MLHR), a type of acoustic metamaterial utilizing Helmholtz resonance across multiple layers, are of particular interest due to their high sound absorption efficiency at minimal material thickness. The sound absorption mechanism of MLHR operates by the intense sound wave vibrations at the narrow necks of each resonant cavity, where frictional dissipation occurs, effectively converting the sound energy into heat and enhancing absorption across a range of frequencies. Traditionally, common types of meta-structures adopting the MLHR mechanism include space-coiling structures [6–8], perforated sandwich panels [9–11], and novel structures such as concentric structures [12], etc (Fig. 1).

Recently, a subclass of MLHR acoustic metamaterials that gained increasing attention due to advances in additive manufacturing technologies is the lattice structure, which is a three-dimensional structure made of repeating units of smaller sub-structures called unit cells (Fig. 1). Due to the unlimited design freedoms associated with unit cells,

* Corresponding author.
E-mail address: xinwei.li@newcastle.ac.uk (X. Li).

https://doi.org/10.1016/j.smmf.2025.100073
Received 31 October 2024; Received in revised form 21 January 2025; Accepted 21 January 2025
Available online 31 January 2025

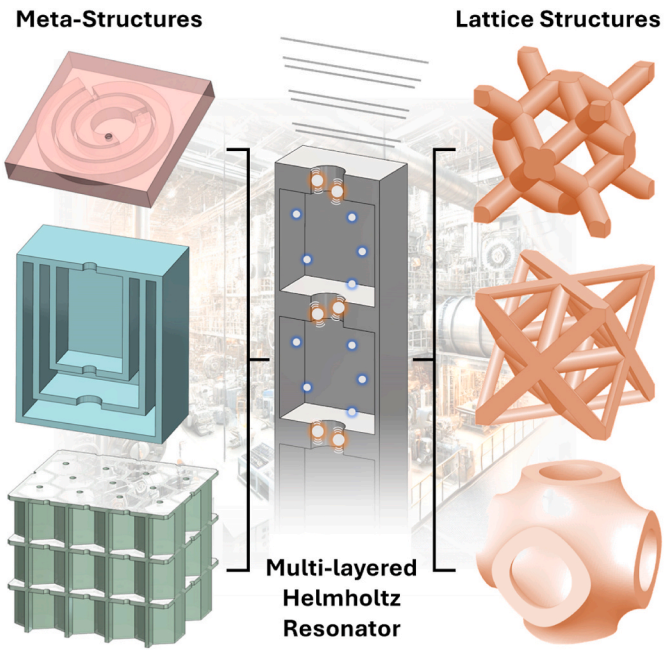

Fig. 1. Schematic illustration of an MLHR, and meta-structures and lattice structures that function based on the MLHR mechanism.

there are many subclasses of lattice structures that have been fabricated and studied for their acoustic properties, including those made of struts [13–15], plates [16–18], shells [19–22] and hybrids [23–26] of the above constituent components. It was worth noting that some lattice designs may be seen as alternating layers of narrow regions and large air cavities which highly resembles the general structure of MLHRs. Indeed, a series of studies by Li et al. [15,16,27,28] suggest that the acoustic properties of some lattice designs, such as those containing struts or perforated plates, may be modeled in a similar way to MLHR [29,30]. A key characteristic of the sound absorption of some of these lattices is the alternating frequency bands of high and low absorption coefficients, with coefficients close to one for some narrow frequency bands [14,16], much unlike the smooth and gradual absorption curves of many foams and fibrous materials. More notably, the acoustic properties of these structures may be tuned towards specific applications through the series or parallel arrangements of unit cells with distinctly different geometries. Despite these potentials, the structure-property relationships between the geometrical factors and sound absorption performance of MLHR-based acoustic metamaterials remain insufficiently understood, posing a challenge in the design phase.

This work addresses this knowledge gap by proposing a generalized MLHR structure-property relationship across a broad range of geometric parameters — specifically, pore diameter (0.9–1.4 mm), pore thickness (1–3 mm), cavity depth (3–7 mm), and number of layers in the MLHR metastructure (2–10). These parameter ranges cover the geometrical parameters commonly used to design MLHR-based metamaterials in practical acoustical applications, thus ensuring that the observed effects and interactions are relevant to a wide design space. Using selected data points, the structural-property relationships in MLHRs for sound absorption are comprehensively determined through the Taguchi method. This approach leverages statistical analysis to efficiently identify key geometric influences and their interactions, requiring only a minimal number of experimental cases. The influences of each of these parameters on the mean sound absorption coefficients (SACs) and the number of local maxima in the absorption curves, within a frequency range of 450 Hz and 6400 Hz, were investigated. A clear relationship between the number of layers and the other acoustical parameters were also established. Overall, a clear hierarchy of factors for maximizing sound absorption is shown, with the number of layers having the greatest impact, followed by reducing pore diameter, increasing pore thickness, and deepening the cavity depth. The established relationships enable a more informed and focused approach to designing MLHRs and other acoustical metamaterials with similar functionality, allowing for the achievement of desired performance targets.

2. Materials and methods

2.1. MLHR design

A schematic of an MLHR is shown in Fig. 2 (A). Each layer of the MLHR contains a two-dimensional array of pores on a flat plate with a cavity beneath. Multiple layers of the same geometrical design may be arranged in series to form the MLHR. Thin pillars were introduced to the design to ensure the plates being held in place. There is virtually no influence on sound absorption by the introduction of these pillars in the cavity, as affirmed in a study in Ref. [28]. For each layer of the MLHR, three independent geometrical variables influence the sound absorption properties of the MLHR, namely the pore diameter (d), pore thickness (t) and cavity depth (D). In this study, we set the cell size to a 5 mm square, which determines the spacing between each pore — and is consistent with the typical size range of common acoustic metamaterials. With the cell size fixed, the influence of surface porosity is effectively represented by the pore diameter alone. Together with the number of layers (N) along the sound propagation direction, these four geometrical variables determine the sound absorption performance of MLHRs.

Out of the four geometrical variables, the effect of the number of layers of the MLHR on the sound absorption properties forms the focus of this study, as the variations in the other geometrical variables on acoustic absorption were widely studied in the literature. Therefore, for every experiment case in this work, the measurements of the sound absorption coefficients were tested across five different layer configurations. The specific values of the four geometrical variables for the MLHR in this work are appended in Table 1.

2.2. Taguchi method

It was noted from Table 1 that for every layer configuration for the MLHR, there are six levels of variables for the pore diameter and three levels each for pore thickness and cavity depth. A full factorial experimental design, which tests all possible combinations of variable levels, would output a total of 270 experiment runs which would be too cost- and time-intensive for a parametric study. Hence, the parametric study on the geometrical variables of the MLHR was done using Taguchi's method [31], which is a robust design methodology for product quality control. Here, the pore diameter, pore thickness, and cavity depth were designated as control factors as these were the most important factors to control when designing for sound absorption purposes. The number of layers of the MLHR was designated as the noise factor as all five levels were required to be tested for each combination. The response variables to be considered in this work were the sound absorption coefficients (SACs) and the number of absorption peaks between a frequency range of 450 Hz and 6400 Hz.

One of the most important steps of the Taguchi method involves the use of orthogonal arrays to represent the factors and levels to be tested in an experiment. These are experiment designs that are reminiscent of fractional factorial experiment designs and leverage orthogonal properties to minimize the number of experiment runs to obtain the required statistical information. In this work, an inner orthogonal array was used to represent the experiment runs that analyze the effects of the control factors on the response variable, mainly the sound absorption coefficients. By referring to a library of orthogonal arrays developed by Taguchi, it was desired that an L18 (6^1) (3^2) orthogonal array would be used in this parametric study of the control variables, as shown in Table 2.

In a Taguchi-designed experiment, the influence of a noise factor can

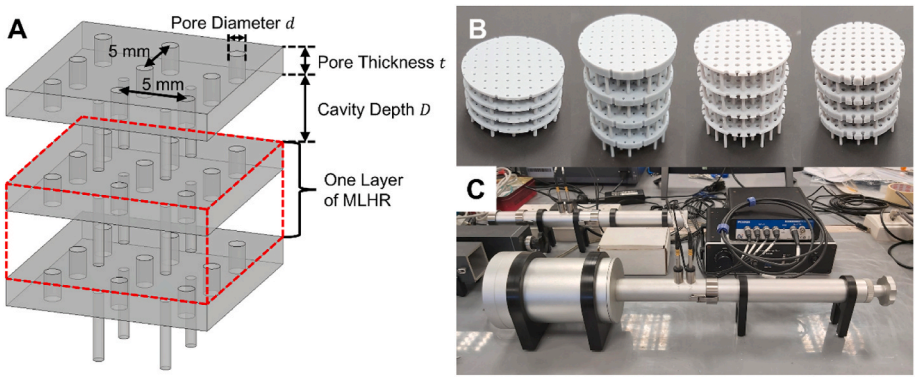

Fig. 2. (A) Schematic of a Multi-Layered Helmholtz Resonator (MLHR) and the key geometrical variables. (B) Photographs of selected MLHR samples fabricated using vat photopolymerization. (C) Photograph of the impedance tube and data acquisition system.

Table 1
Values of geometrical variables in the parametric study.

Geometrical Variable	Units	Type of Factor	Values
Pore Diameter d	mm	Control	0.9, 1.0, 1.1, 1.2, 1.3, 1.4
Pore Thickness t	mm	Control	1, 2, 3
Cavity Depth D	mm	Control	3, 5, 7
Number of Layers N	No Units	Noise	2, 4, 6, 8, 10

Table 2
The inner orthogonal array showing values of geometrical variables in each experiment.

Experiment No.	Pore diameter (mm)	Pore thickness (mm)	Cavity depth (mm)
1	0.9	1	3
2	0.9	2	5
3	0.9	3	7
4	1	1	3
5	1	2	5
6	1	3	7
7	1.1	1	5
8	1.1	2	7
9	1.1	3	3
10	1.2	1	7
11	1.2	2	3
12	1.2	3	5
13	1.3	1	5
14	1.3	2	7
15	1.3	3	3
16	1.4	1	7
17	1.4	2	3
18	1.4	3	5

be desired or undesired depending on the objective of the experiment. Since the number of layers is one of the key structural variables in determining the sound absorption performance of the MLHRs, its influence on the sound absorption performance is desired. Hence, all five levels for the number of layers were included in the outer array for the experiment table such that every experiment case in Table 2 was run five times with each of the different number of layers. Moreover, as the effects of the control factors on the response would be confounded by the number of layers of the MLHR, the interactions between the control factors and the noise factor were analyzed using the signal-to-noise ratio (S/N ratio). As higher acoustic absorption performances for the MLHRs were desired in practical settings, the S/N ratio was calculated based on the "larger the better" situation, as follows:

$$S\Big/N = -10\log\frac{1}{n}\sum_{i=1}^{n}\frac{1}{Y_i^2}, \tag{1}$$

where n is the number of experiment runs at the outer array and Y_i is the response variable for the i^{th} experiment run. It is important to note that higher S/N ratios signify control factor levels that maximize the influence of the noise factor on the dependent variables.

2.3. Fabrication of MLHRs

The MLHRs in this work were fabricated using the vat photopolymerization process with polymer resin. The vat photopolymerization machine used in this work is the Asiga Max X27, which manufactures the sample layer-by-layer by selective curing of the liquid resin. The resolution of the printer was 27 μm which was sufficiently small for the accurate manufacturing of the small dimensions required for this work. A layer thickness of 0.05 mm, light intensity of 10 mW/cm^{2,} and exposure time of 1 s were used during printing. Samples of circular cross-sections with a sample diameter of 29 mm were fabricated. As-printed parts were cleaned by immersing them in isopropyl alcohol for about 20 min and then dried and post-cured in a UV curing chamber for about 30 min. Photographs of selected representative samples fabricated for this work are shown in Fig. 2 (B).

2.4. Acoustic performance characterization

The SAC of the printed MLHR samples was measured experimentally using the BSWA SW4601 tube, shown in Fig. 2 (C), based on the ASTM E1050 – 19 standards. The sample holder has a hole diameter of 29 mm and the samples were fully inserted into the holder with minimal air gaps at the walls of the holder. The frequency range of interest is between 450 Hz and 6400 Hz.

3. Results and discussions

3.1. Sound absorption properties of MLHRs

Fig. 3 shows the plots of SACs for two different experiment cases with varying numbers of layers. Fig. 3(A) shows those for Experiment 1 and Fig. 3(B) shows those for Experiment 18. The plots for the other experiment cases listed in Table 2 are included in Figs. S1–3 in the Supplementary Materials. These two experiment cases were chosen due to the large differences in control factors, allowing for an overview of the possible variations in SAC trends within the parametric study. It was observed from the figures that as the number of layers along the sound propagation direction increases, both the average sound absorption coefficient and the number of absorption peaks increase. For example, for Experiment 1, the average absorption coefficient changes from 0.278 to 0.552, and the peak count increases from 1 to 3 as the number of layers increases from 2 to 10. These findings align with our hypothesis that increasing the number of layers of an MLHR allows the structure to

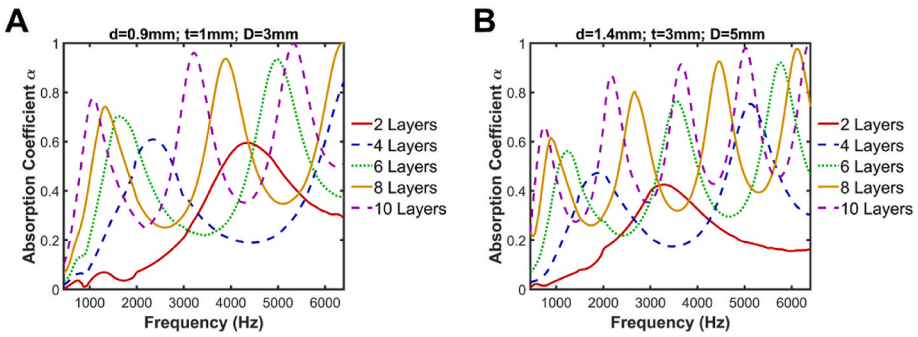

Fig. 3. Plot of the variations in sound absorption coefficients with the number of layers for (A) Experiment 1 and (B) Experiment 18.

dissipate more sound energy, a boarder spectrum of frequencies could therefore be absorbed. Also, the increase in the number of layers generally shifts the first absorption peaks to lower frequencies. This was due to the increase in distance when sound waves travel within the cavities, leading to stronger interactions between the lattice structure and the sound waves that are periodically longer. When comparing Experiments 1 and 18, it was observed that the mean SACs were largely similar but Experiment 18 showed a larger number of absorption peaks, and the frequencies of the first absorption peaks were lower than those in Experiment 1. The effects of the three control factors on the mean absorption coefficients and the number of absorption peaks will be discussed in the following subsections.

3.2. *Effects of geometry on mean SAC*

Fig. 4 (A) shows the variations in mean SAC with the various geometrical variables in Table 1. An increase in pore diameter was associated with a decrease in mean SAC, while an increase in pore thickness, cavity depth, or number of layers was associated with an increase in mean SAC. These results were mostly similar to other works in the literature which suggested that an increase in mean SACs could be achieved by using pores with smaller diameters and longer thicknesses and using cavities with larger depth [32,33]. The increase in the number of layers of the MLHR means that acoustic energy may be dissipated over a larger number of pore-cavity pairs, hence the increase in mean SAC was expected [33].

To determine if changes to the control factors would lead to a change in mean SACs for the MLHR, a 3-way analysis of variance (ANOVA) was conducted and the p-values obtained were plotted in Fig. 4 (B). In the 3-way ANOVA, the null hypothesis was that the mean SACs of the MLHR were unaffected by changes in the control factors. The p-values obtained from the analysis indicate the probability of obtaining the SACs in the experiment given the null hypothesis was true. Most p-values obtained from the ANOVA were below 5% which suggests that there was sufficient evidence to reject the null hypothesis at a 5% level of significance that the changes in control factors do not affect the mean SACs. Therefore, given the number of layers of the MLHR was fixed, the mean SACs were significantly affected by changes in pore diameter, pore thickness, and cavity depth. The only exception was the effect of cavity depth on the mean SACs of a two-layer MLHR. This means that for an MLHR with two layers, the cavity depth may play a minimal role in changing the mean SACs as compared to the pore diameter and pore thickness.

Finally, knowing that the effects of the three control factors on the mean SACs were significant, the correlations between the control factors

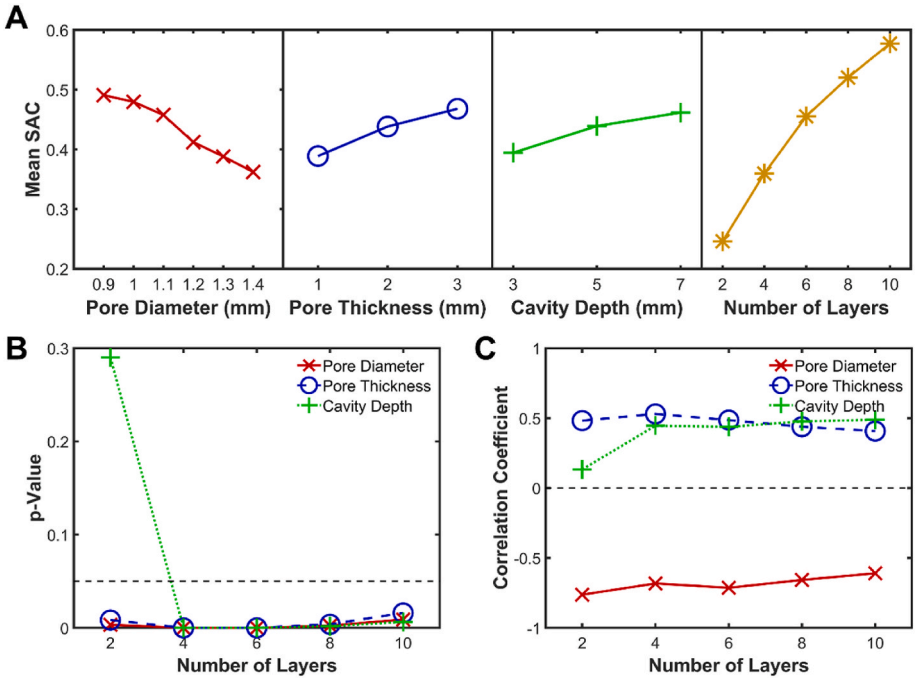

Fig. 4. (A) Plot of the variations in mean sound absorption coefficients with the geometrical parameters in Table 1. (B) Plot of the variations in p-values obtained from analysis of variance (ANOVA) with the number of layers. (C) Plots of the variations in correlation coefficients between the control variables and the SAC with the number of layers.

and the mean SACs were investigated, with the number of layers fixed. Fig. 4 (C) shows the variations in correlation coefficients between the control variables and the SAC with the number of layers. It was important to note that the magnitude of the correlation coefficient signifies the strength of linear correlation between the control variables and the mean SACs, while the sign indicates the direction of correlation. It was noted that the correlation between pore diameter and the mean SACs was the strongest among the three control variables with a moderate negative mean correlation coefficient of about −0.685. The correlations between pore thickness or cavity depth and mean SACs were positive and moderate to weak at 0.469 and 0.396 respectively. The low correlation between the cavity depth and the mean SACs for a 2-layer MLHR was notable due to the lack of influence of changes in cavity depth on mean SACs as noted in Fig. 4 (B). Moreover, as the number of layers of the MLHR was changed, slight variations in the correlation coefficients were reported while the direction of correlations remained unchanged. Hence, it can be concluded that the pore diameter was negatively correlated with mean SACs, and pore thickness and cavity depth were positively correlated with mean SACs. Furthermore, the number of layers of the MLHR may pose minimal effects on the correlation between the control factors and the mean SACs.

At this point, the correlations between the control factors and the mean SAC were established while keeping the number of layers fixed. This work then proceeds to identify the relationships between the number of layers on the mean SAC and how the number of layers influences the correlations between the control factors and the mean SAC. Fig. 5 (A) shows the variations in correlation coefficients between the number of layers and the mean SAC, keeping each of the control factors constant. Here, it was obvious that there was a strong positive correlation between the number of layers and the mean SAC, with correlation coefficients mostly around 0.9. The magnitude of correlation coefficients was observed to decrease with increasing pore diameter, increasing pore thickness, or increasing cavity depth. However, the strength of correlation between the number of layers and the mean SAC was still strong. Hence, we can conclude that increasing the number of layers of an MLHR will increase the mean SAC.

Fig. 5 (B) shows the variations in the mean S/N ratio with the various control factors. A larger S/N ratio means that changing the number of layers of the MLHR has a larger influence on the mean SAC. It was observed that the S/N ratio was largest when the pore diameter was smaller, the pore thickness was larger and the cavity depth was larger. Based on the discussions of the results in Fig. 4, we can also imply that the changes in control factors towards higher mean SACs also increase the number of layers on the mean SAC of the MLHR. It was also noted that the SN ratio changes with the control factors, which means that changing the control factors also changes the sensitivity of the mean SAC of the MLHR to changes in the number of layers. Based on the ranges of control factors studied, it was observed that the changes in the S/N ratio were largest when the pore diameter was changed, followed by the pore thickness and cavity depth. Overall, we can conclude that changing the geometrical parameters towards higher mean SACs also increases the sensitivity of the mean SAC to changes in the number of layers, while changes in geometrical parameters towards lower mean SACs also lower the sensitivity of the mean SACs to changes in the number of layers. Intuitively, this means when a trial MLHR design has mean SACs lower than expected, adding more layers to the MLHR may have less effect of increasing the mean SACs as compared to decreasing the pore diameter or increasing the pore thickness or cavity depth.

3.3. *Effects of geometry on the number of absorption peaks*

In this subsection, the effects and correlations between the control and noise factors and the number of absorption peaks between 450 Hz and 6400 Hz were investigated similarly. Fig. 6 (A) shows the variations in the geometrical factors with the average number of absorption peaks. The values were obtained by obtaining the average number of absorption peaks of experiment cases for fixed values of a particular geometrical parameter. When compared with Fig. 4 (A), it was observed that

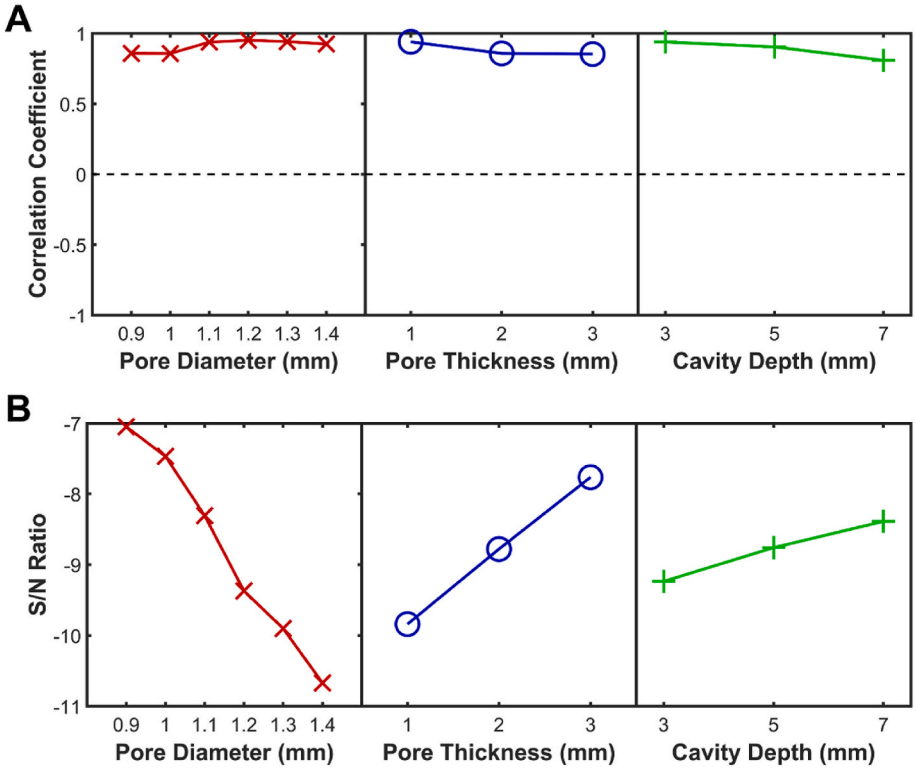

Fig. 5. (A) Plots of the variations in correlation coefficients between the number of layers and the SAC with the control variables in Table 1. (B) Plots of the variations in signal-to-noise ratios with the control variables in Table 1.

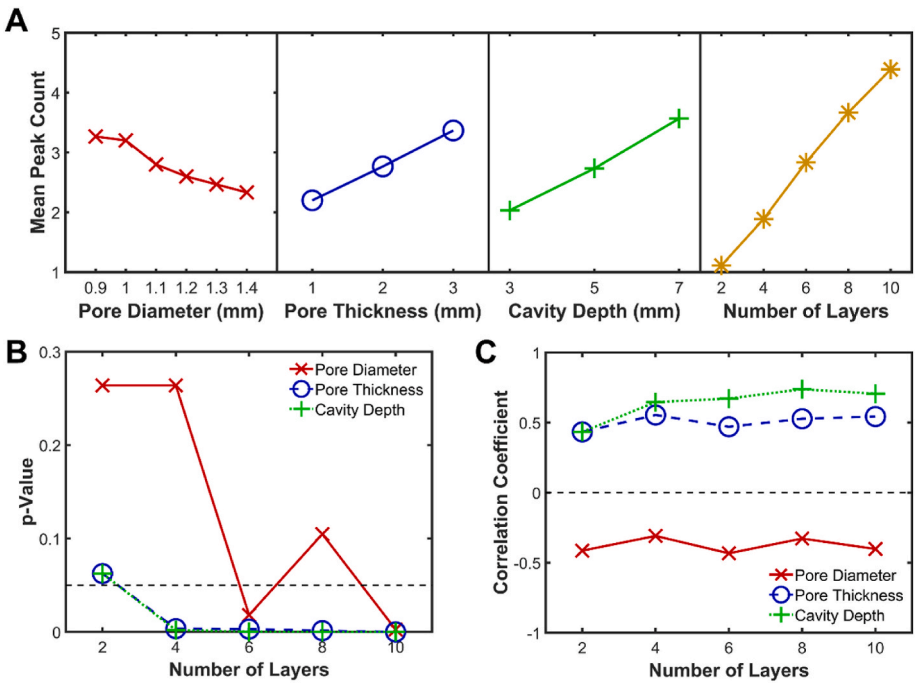

Fig. 6. (A) Plot of the variations in the average number of peaks with the geometrical parameters in Table 1. (B) Plot of the variations in p-values obtained from analysis of variance (ANOVA) with the number of layers. (C) Plots of the variations in correlation coefficients between the control variables and the number of absorption peaks with the number of layers.

changes in the geometrical factors that increase the mean SAC of the MLHRs also increase the number of absorption peaks. It is important to note that the increase in the mean SAC of an MLHR does not necessarily lead to an increase in the number of absorption peaks within the same frequency range. However, we observe from the plots of sound absorption coefficients with frequency that the MLHRs with higher mean SACs also tend to exhibit more periodic behavior. Unlike the mean SACs, the change in pore thickness has less effect on changing the number of peaks as compared to changing the cavity depth. The greater influence of cavity depth on the number of peaks can be inferred in a mathematical sense when modeling the acoustic properties of the air cavity layer. Due to the use of $\cos(kD)$ and $\sin(kD)$ functions to represent plane waves travelling within the cavity layer, the period of the waves tends to become smaller due to larger cavity depth D.

Next, to determine the effects of the control factors on the number of absorption peaks, a 3-way analysis of variance (ANOVA) was conducted and the p-values obtained were plotted in Fig. 6 (B). The results obtained vary significantly from the 3-way ANOVA results in Fig. 4 (B) due to the different ways the factors act on the mean SAC as compared to the number of absorption peaks. For a 2-layer MLHR, the p-values were larger than 0.05, which means that there was insufficient evidence to reject the hypothesis at 5% level of significance that the number of peaks was unaffected by changes to the control factors. This was understandable as the overall height of the MLHRs would be very small such that the wavelengths of the acoustic waves become more comparable to the MLHR dimensions. With more than 2 layers, the p-values for pore thickness and cavity depth were extremely small while the p-values for pore diameter may or may not be smaller than 0.05. Therefore, there was sufficient evidence to conclude the number of absorption peaks is affected by pore thickness and cavity depth, while there was insufficient evidence to determine whether the effects of pore diameter on the number of absorption peaks were significant.

Furthermore, it was found that the variations in correlation coefficients between the control factors and the number of absorption peaks, plotted in Fig. 6 (C), were mostly similar to those for mean SACs with some variations. Firstly, the magnitudes of correlation coefficients between the pore diameter and the number of absorption peaks were lower, suggesting a weak correlation between the pore diameter and the number of absorption peaks. Also, the magnitudes of correlation coefficients between the cavity depth and the number of absorption peaks were now moderate and positive, which further strengthens the claim that changing the cavity depth has a larger effect on the number of absorption peaks of an MLHR.

Fig. 7 (A) shows the variations in correlation coefficients between the number of layers and the number of absorption local maxima, keeping each of the control factors constant. Similar to the mean SACs, there was a strong positive correlation between the number of layers and the number of absorption peaks, with correlation coefficients mostly around 0.9. The magnitude of correlation coefficients was observed to decrease with increasing pore diameter, increasing pore thickness, or increasing cavity depth. Due to the strength of correlations being very strong, it can be concluded with confidence that the increase in the number of layers of an MLHR will increase the number of absorption peaks in addition to increasing the mean SACs.

Fig. 7 (B) shows the variations in the mean S/N ratio for the number of absorption peaks with the various control factors. Similarly to Fig. 5, a larger S/N ratio means that changing the number of layers of the MLHR has a larger influence on the number of absorption peaks. It was observed that the S/N ratio was largest when the pore diameter was smaller, the pore thickness was larger and the cavity depth was larger. Based on the discussions of the results in Fig. 4, we can also imply that the changes in control factors towards a higher number of absorption peaks also increase the influence of the number of layers on the number of absorption peaks of the MLHR. It was also noted that the S/N ratio changes with the control factors, which means that changing the control factors also changes the sensitivity of the number of absorption peaks of the MLHR to changes in the number of layers. Based on the ranges of control factors studied, it was observed that the changes in the S/N ratio were largest when the cavity width was changed, followed by the pore thickness and pore diameter. Overall, we can conclude that changing the geometrical parameters towards a higher number of absorption peaks also increases the sensitivity of the number of absorption peaks to

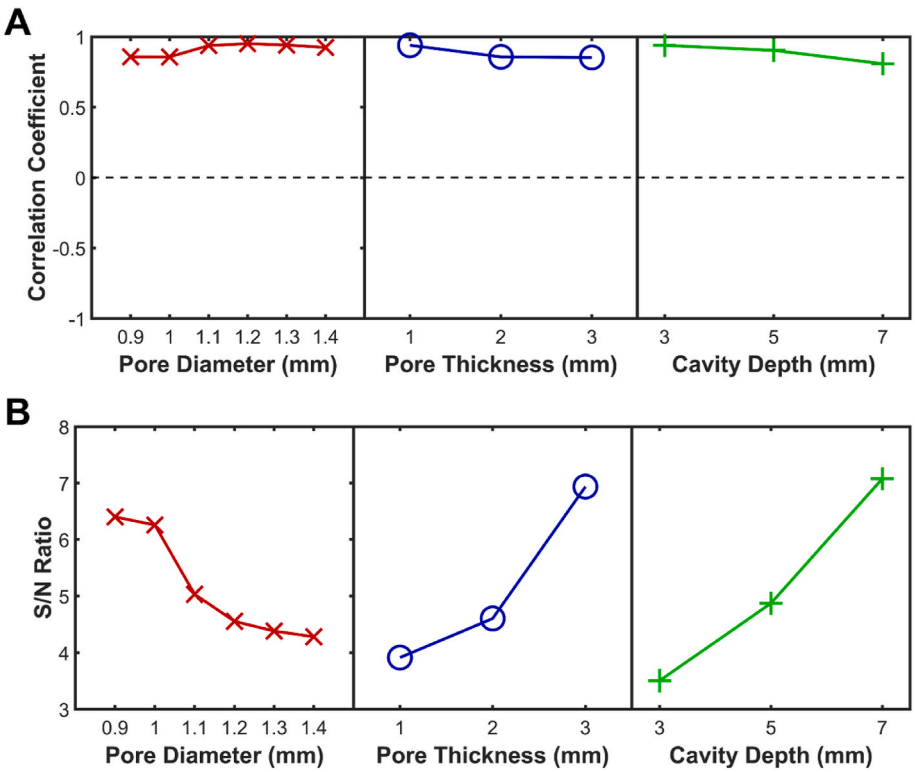

Fig. 7. (A) Plots of the variations in correlation coefficients between the number of layers and the number of absorption peaks with the control variables in Table 1. (B) Plots of the variations in signal-to-noise ratios with the control variables in Table 1.

changes in the number of layers, while changes in geometrical parameters towards the lower number of absorption peaks also lower the sensitivity of the number of absorption peaks to changes in the number of layers.

3.4. *Summary of findings*

Table 3 summarizes the directions and strengths of correlations between the geometrical factors and the average SACs and the number of absorption peaks of the MLHRs. It was shown that the pore diameter exhibited a negative correlation with both the mean SACs and the number of absorption peaks. Both the pore thickness and cavity width showed a positive correlation with the mean SACs and the number of absorption peaks. Most of the correlations between the control factors and the response variables were moderate with two notable exceptions. The pore diameter showed weak correlations with the number of absorption peaks while the cavity width exhibited weak correlations with the mean SACs. The number of layers of the MLHR showed strong positive correlations with both response variables, with the increase in the number of layers almost surely leading to an increase in mean SACs and the number of absorption peaks. The observations for the S/N ratios from the work were summarized in Table 4. It was noted that the sensitivity of both response variables to changes in the number of layers was higher with smaller pore diameters, larger pore thickness, or larger cavity depths, which also corresponds to directions of increasing mean SACs and number of absorption maxima. The sensitivity of the mean SACs to changes in number of layers was largest with changes in pore diameter, followed by pore thickness and cavity width, while the sensitivity of the number of absorption peaks to changes in number of layers was largest with changes in cavity width, followed by pore thickness and pore diameter.

Table 3
Summary of directions and strengths of correlations.

Geometrical Variables	Average SACs		Number of Absorption Peaks	
	Correlation	Rank	Correlation	Rank
Pore Diameter	Negative, Moderate (−0.685)	2	Negative, Weak (−0.377)	4
Pore Thickness	Positive, Moderate (0.469)	3	Positive, Moderate (0.505)	3
Cavity Depth	Positive, Weak (0.396)	4	Positive, Moderate (0.639)	2
Number of Layers	Positive, Strong (0.897)	1	Positive, Strong (0.840)	1

The ranks shown in this table show the comparative strength of influence of changing the geometrical variable on the response. The higher the rank, the greater the influence.

4. Further discussions

In this work, the interactions between the geometrical factors (pore diameter, pore thickness, cavity width, and number of layers) of the MLHR and the response variables (mean SAC and number of absorption peaks) were investigated using the Taguchi method. Conventional parametric experiments involve the use of several variables with multiple levels, followed by side-by-side comparisons of experimental results with only one variable changed and keeping the others constant.

Table 4
Summary of signal-to-noise (S/N) ratios.

Geometrical Variables	Average SACs		Number of Absorption Peaks	
	Direction	Rank	Direction	Rank
Pore Diameter	Decrease	1	Decrease	3
Pore Thickness	Increase	2	Increase	2
Cavity Depth	Increase	3	Increase	1

Remarks: This table tells us whether to increase or decrease the values of the independent variables to maximize the influence of the number of layers on the dependent variables.

Such approaches would either involve a lot of experiment work due to the use of full-factorial experiment design or provide limited information if pairwise comparisons were done around a certain center case. Additionally, some other works focused on adopting theoretical MLHR models to categorize sound absorption properties [15,28,32]. However, a key limitation of MLHR theoretical models is their reliance on experimental data to determine end correction parameters, which introduces an empirical aspect to achieving high-fidelity numerical models. Often at times, the end correction parameters are also dependent on the actual metamaterial geometry, such as the pore and cavity morphology. Our work herein focused on directly analyzing the influence of geometric parameters on sound absorption via experimental data. While numerical models provide valuable insights, experimentally-derived data remains more conclusive when establishing structural-property relationships. The Taguchi method in this work provides a quantitative way of expressing the inter-relationship between variables through correlation coefficient calculations and S/N ratios.

Through the use of statistical metrics and methods, we were able to determine how the number of layers of an MLHR influences the magnitudes of the response variables (Fig. 4 (A) and Fig. 5 (A)), how the number of layers affects the ways the other control variables interact with the response variables (Fig. 4(B) and (C)), and how does the control variables influence how much the number of layers affect the responses (Fig. 5 (B)). These detailed structure-property relationships may be leveraged in the design of MLHRs for targeted design specifications. For instance, to design an MLHR with high overall SACs, the structural-property relationships tell us that such an objective may be achieved by performing the following tweaks to the geometrical variables, in the following order of importance (Fig. 8).

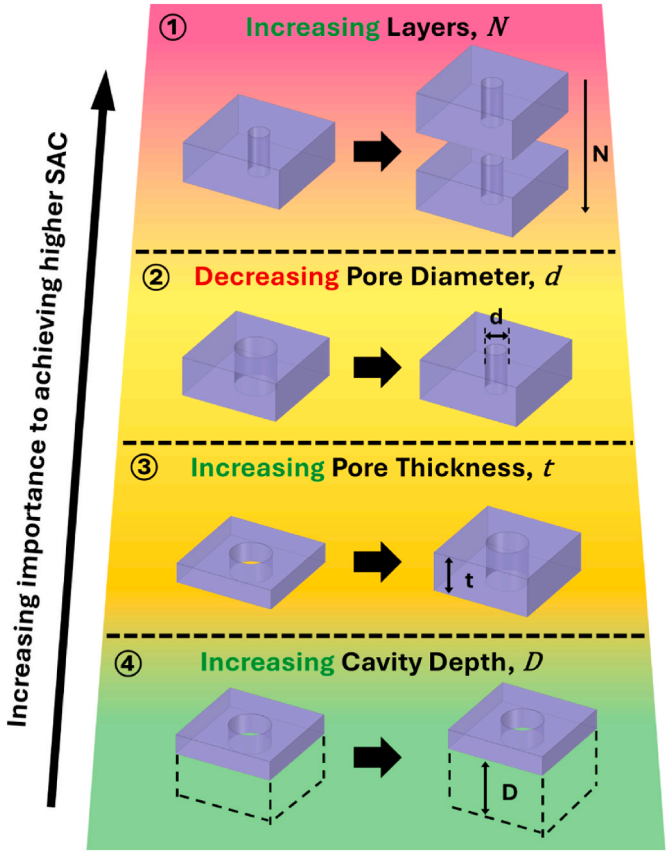

Fig. 8. An overview of the structural-property relationship between the geometrical parameters and achieving high SAC.

1. Increasing the number of layers: Adding more layers to the structure increases the pathways through which sound waves must travel, effectively creating a multi-resonant system. Each layer introduces additional channels for sound wave dissipation owing to frictional losses. Multi-layered structures also constitute additional resonance states, effectively adding more resonance peaks which then increases the average SAC.
2. Reducing pore diameter: Smaller pore diameters increase the resistance to airflow as sound waves enter the structure, resulting in higher "drag" forces from the walls and thus higher viscous frictional losses.
3. Increasing pore thickness: Increasing the pore thickness leads to increased rigidity and mass of the Helmholtz resonator. This added mass leads to increased inertia, meaning that sound energy is "trapped" within the cavity for longer, allowing more time for energy dissipation. Additionally, thicker pores constitute increased solid material for interaction with sound waves, effectively enhancing frictional losses and sound wave dissipation.
4. Increasing cavity depth: Cavity depth primarily controls the frequency at which resonance occurs. The cavity depth is directly related to the wavelength of sound it can absorb; deeper cavities are more effective at capturing lower-frequency sound waves, which have longer wavelengths.

The structure-property relationships obtained for the MLHRs in this work may be readily expanded to resonant-based acoustic metamaterials that comprise alternating layers of narrow pores or tubes and air cavities. As mentioned in the introduction, there are numerous instances of acoustic metamaterials designed leveraging the principle of MLHR to achieve broadband sound absorption. The multi-functional resonant-based lattice sound absorbers are noteworthy due to the inherent use of repeating units of unit cells functioning on resonance in the design [16–18,26,34]. Most conventional strut lattices such as the simple-cubic and Kelvin-cell lattices tend to contain struts that form several closed loops that bear some resemblance to narrow pores while encasing one or more large cavity volumes within the cells [15]. For plate lattices, some researchers leverage the inclusion of drain holes on the plates to remove excess material during additive manufacturing, while acting as narrow pores similar to those of perforated plates. The pores that remain within the lattices then act as the cavity volumes adjacent to the pores, resulting in an interconnected system of pores and cavities similar to an MLHR [16]. While the multi-functionalities of the lattice structures were proven in detail in the respective journal articles, this work aims to paint a better picture of how these lattice structures may be better designed by making clever use of the structure-property relationships of MLHRs.

5. Conclusions

In this work, we conducted a parametric study to unveil the structure-property relationships between various geometrical factors and the sound absorption properties of MLHRs. The pore diameter (d), pore thickness (t) and cavity depth (D) were designated control factors, while the number of layers of the MLHR (N) was designated as the noise factor. The experiments for the control factors were designed using an inner orthogonal array which offers sufficient data for statistical analysis with much fewer experiments as compared to a typical full-factorial experiment design. The strengths and directions of correlations between the geometrical parameters and the responses were summarized in Table 3. The observations for the S/N ratios from the work were summarized in Table 4. The derived relationships allow for a more informed and targeted approach to the design of MLHRs and several acoustic metamaterials functioning similarly to MLHRs to achieve target design specifications for practical acoustics applications.

CRediT authorship contribution statement

Jun Wei Chua: Writing – original draft, Visualization, Validation, Supervision, Software, Methodology, Investigation, Formal analysis, Data curation. **David Kar Wei Poh:** Visualization, Validation, Software, Methodology, Investigation, Formal analysis, Data curation, Conceptualization. **Shuwei Ding:** Visualization, Validation, Supervision, Software, Investigation, Formal analysis. **Haoran Pei:** Visualization, Validation, Supervision, Software, Investigation, Formal analysis, Data curation. **Xinwei Li:** Writing – review & editing, Supervision, Software, Project administration, Methodology, Funding acquisition, Conceptualization.

Data availability statement

The data that support the findings of this study are available on request from the corresponding author.

Declaration of competing interest

The authors declare that they have no known competing financial interests or personal relationships that could have appeared to influence the work reported in this paper.

Acknowledgments

This work was supported by the MOE AcRF Tier 1 Grant (project no. WBS A-8002418-00-00).

Appendix A. Supplementary data

Supplementary data to this article can be found online at https://doi.org/10.1016/j.smmf.2025.100073.

References

[1] H.T. Diong, R. Neitzel, W.H. Martin, Spatial evaluation of environmental noise with the use of participatory sensing system in Singapore, Noise Mapp. 8 (1) (2021) 236–248.
[2] H.J. Jariwala, H.S. Syed, M.J. Pandya, Y.M. Gajera, Noise Pollution & Human Health: A Review, Noise and Air Pollution: Challenges and Opportunities, 2017.
[3] Acoustic Insulation Market Size, Share & Trends Analysis Report by Product, by End-Use, by Region (North America, Europe, APAC, Central & South America, MEA), and Segment Forecasts, 2016 - 2025, Market Analysis Report, Grand View Research, 2016.
[4] M. Yang, P. Sheng, Sound absorption structures: from porous media to acoustic metamaterials, Annu. Rev. Mater. Res. 47 (2017) 83–114.
[5] F. Zangeneh-Nejad, R. Fleury, Active times for acoustic metamaterials, Reviews in Physics 4 (2019).
[6] H. Ryoo, W. Jeon, Perfect sound absorption of ultra-thin metasurface based on hybrid resonance and space-coiling, Appl. Phys. Lett. 113 (12) (2018).
[7] J.-S. Chen, Y.-B. Chen, Y.-H. Cheng, L.-C. Chou, A sound absorption panel containing coiled Helmholtz resonators, Phys. Lett. 384 (35) (2020) 126887.
[8] Q. Xu, J. Qiao, G. Zhang, L. Li, Low-frequency sound-absorbing metasurface constructed by a membrane-covered and coiled Helmholtz resonator, J. Appl. Phys. 133 (7) (2023).
[9] Y. Tang, F. Li, F. Xin, T.J. Lu, Heterogeneously perforated honeycomb-corrugation hybrid sandwich panel as sound absorber, Mater. Des. 134 (2017) 502–512.
[10] W. He, X. Peng, F. Xin, T.J. Lu, Ultralight micro-perforated sandwich panel with hierarchical honeycomb core for sound absorption, J. Sandw. Struct. Mater. (2021) 1099636221993880.
[11] H. Duan, X. Shen, E. Wang, F. Yang, X. Zhang, Q. Yin, Acoustic multi-layer Helmholtz resonance metamaterials with multiple adjustable absorption peaks, Appl. Phys. Lett. 118 (24) (2021).
[12] J.-M. Coulon, N. Atalla, A. Desrochers, Optimization of concentric array resonators for wide band noise reduction, Appl. Acoust. 113 (2016) 109–115.
[13] J. Liu, T. Chen, Y. Zhang, G. Wen, Q. Qing, H. Wang, R. Sedaghati, Y.M. Xie, On sound insulation of pyramidal lattice sandwich structure, Compos. Struct. 208 (2019) 385–394.
[14] D.H. Kassim, A. Putra, M.F.S.C. Hamid, M.R. Alkahari, in: U. Sabino, F. Imaduddin, A.R. Prabowo (Eds.), Sound Absorption of BCC Lattice Structures, Springer, 2020, pp. 69–79.
[15] J.W. Chua, Z. Lai, X. Li, W. Zhai, LattSAC: a software for the acoustic modelling of lattice sound absorbers, Virtual Phys. Prototyp. 19 (1) (2024).
[16] X. Li, X. Yu, J.W. Chua, H.P. Lee, J. Ding, W. Zhai, Microlattice metamaterials with simultaneous superior acoustic and mechanical energy absorption, Small 17 (24) (2021) e2100336.
[17] Z. Li, W. Zhai, X. Li, X. Yu, Z. Guo, Z. Wang, Additively manufactured dual-functional metamaterials with customisable mechanical and sound-absorbing properties, Virtual Phys. Prototyp. 17 (4) (2022) 864–880.
[18] L. Li, F. Yang, Y. Jin, P. Li, S. Zhang, K. Xue, G. Lu, H. Fan, Multifunctional hybrid plate lattice structure with high energy absorption and excellent sound absorption, Mater. Des. 241 (2024).
[19] F.S.L. Bobbert, K. Lietaert, A.A. Eftekhari, B. Pouran, S.M. Ahmadi, H. Weinans, A. A. Zadpoor, Additively manufactured metallic porous biomaterials based on minimal surfaces: a unique combination of topological, mechanical, and mass transport properties, Acta Biomater. 53 (2017) 572–584.
[20] W. Yang, J. An, C.K. Chua, K. Zhou, Acoustic absorptions of multifunctional polymeric cellular structures based on triply periodic minimal surfaces fabricated by stereolithography, Virtual Phys. Prototyp. 15 (2) (2020) 242–249.
[21] X.-n. Kong, B. Liu, Z.-H. Li, P.-F. Zhang, C. Shi, Research on sound absorption properties of tri-periodic minimal surface sandwich structure of selective laser melting titanium alloy, Mater. Trans. 64 (4) (2023) 861–868.
[22] J. Feng, J. Qiao, Q. Xu, Y. Wu, G. Zhang, L. Li, Broadband sound absorption and high damage resistance in a turtle shell-inspired multifunctional lattice: neural network-driven design and optimization, Small 20 (42) (2024) e2403254.
[23] Z. Li, X. Wang, X. Li, Z. Wang, W. Zhai, New class of multifunctional bioinspired microlattice with excellent sound absorption, damage tolerance, and high specific strength, ACS Appl. Mater. Interfaces 15 (7) (2023) 9940–9952.
[24] Z. Wang, Z. Guo, Z. Li, K. Zeng, Design, manufacture, and characterisation of hierarchical metamaterials for simultaneous ultra-broadband sound-absorbing and superior mechanical performance, Virtual Phys. Prototyp. 18 (1) (2022).
[25] J.W. Chua, X. Li, X. Yu, W. Zhai, Novel slow-sound lattice absorbers based on the sonic black hole, Compos. Struct. 304 (2023).
[26] L. Li, Z. Guo, F. Yang, P. Li, M. Zhao, Z. Zhong, Additively manufactured acoustic-mechanical multifunctional hybrid lattice structures, Int. J. Mech. Sci. 269 (2024).
[27] X. Li, X. Yu, M. Zhao, Z. Li, Z. Wang, W. Zhai, Multi-level bioinspired microlattice with broadband sound-absorption capabilities and deformation-tolerant compressive response, Adv. Funct. Mater. 33 (2) (2022) 2210160.
[28] X. Li, S. Ding, X. Wang, S.L.A. Tan, W. Zhai, Recipe for simultaneously achieving customizable sound absorption and mechanical properties in lattice structures, Advanced Materials Technologies (2024) 2400517.
[29] A.I. Komkin, M.A. Mironov, A.I. Bykov, Sound absorption by a Helmholtz resonator, Acoust Phys. 63 (4) (2017) 385–392.
[30] D.-Y. Maa, Potential of microperforated panel absorber, J. Acoust. Soc. Am. 104 (5) (1998) 6.
[31] G. Taguchi, S. Chowdhury, Y. Wu, Taguchi's Quality Engineering Handbook, Wiley2004.
[32] X. Li, X. Yu, J.W. Chua, W. Zhai, Harnessing cavity dissipation for enhanced sound absorption in Helmholtz resonance metamaterials, Mater. Horiz. 10 (8) (2023) 2892–2903.
[33] X. Li, X. Yu, W. Zhai, Additively manufactured deformation-recoverable and broadband sound-absorbing microlattice inspired by the concept of traditional perforated panels, Adv. Mater. 33 (44) (2021) 2104552.
[34] Z. Li, X. Li, J.W. Chua, C.H. Lim, X. Yu, Z. Wang, W. Zhai, Architected lightweight, sound-absorbing, and mechanically efficient microlattice metamaterials by digital light processing 3D printing, Virtual Phys. Prototyp. 18 (1) (2023).